Coupling currents and hysteresis losses in MgB_2 superconductors

N Magnusson[1], S Lindau[2], H Taxt[1] and M Runde[1]

[1]SINTEF Energy Research, NO-7465 Trondheim, Norway
[2]Norwegian University of Science and Technology, Department of Electric Power Engineering, NO-7491 Trondheim, Norway

E-mail: niklas.magnusson@sintef.no

Abstract
MgB_2 multi-filamentary superconductors are widely considered for use in dc applications. To expand the possible application range to ac apparatuses, the development of a low ac loss wire is needed. This development involves several steps, and a solid understanding of the loss mechanisms is important to optimize that process as well as for evaluating dc wires exposed to current or magnetic field ripple. In this study we discuss the coupling currents and their influence on hysteresis loss as well as on coupling current loss. We give a phenomenological explanation of the origin and behaviour of the coupling currents and describe the loss patterns for hysteresis loss and coupling current loss separately. Finally, we interpret measured AC losses in an MgB_2 wire cut into different lengths representing different twist pitches. Under certain circumstances short sample lengths are shown to give inaccurate measurement results. On the other hand, short sample lengths of non-twisted wires can be used to estimate the twist pitch necessary to electromagnetically decouple the superconducting filaments.

1. Introduction

At its operating temperature in the 20 - 30 K range, the MgB_2 superconductor brings advantages compared to low-temperature superconductors (LTSs) in terms of lower cooling costs, and compared to high-temperature superconductors (HTSs), like YBCO and BSCCO, in terms of lower wire costs. In this respect it is notable that the MgB_2 wire cost per unit carried current is dramatically lower, a factor of ten or more, than the cost for standard copper conductors. These features have led several groups to consider using MgB_2 conductors in e.g. MRI magnets [1, 2] replacing LTSs, in induction heaters [3] replacing HTSs [4], and in generator rotors [5-8] for large off-shore wind turbines as a cost efficient conductor for a new product.

These are all dc applications. For ac applications, the losses appearing in the presence of an alternating magnetic field need to be considered and kept at a tolerable level. Based on a comparison with the 40 W/kAm of losses in copper conductors carrying 2 A/mm^2 at room temperature , the tolerable losses at 30 K can be estimated to about 0.1 W/kAm taking a cooling penalty factor of 50 and an overall loss reduction (to really gain something) by a factor of 8 into account. This number may vary with the application, and additional benefits the use of superconductors may yield can result in a higher acceptable loss level.

Present commercial MgB_2 wires are made for dc use and experience losses far exceeding 0.1 W/kAm for applications of interest [9]. An obvious reason is the commonly used nickel matrix, leading to magnetic hysteresis losses in the matrix. However, also when using a non-magnetic matrix, like titanium, the losses in standard shaped, non-twisted multi-filamentary wires are high, well above 1 W/kAm at 0.1 T [10]. To expand the MgB_2 market to cover also ac applications, the losses have to be dramatically reduced. The route towards a low ac loss multi-filamentary MgB_2 wire (with a nonmagnetic matrix) includes filament twisting and insertion of high resistivity matrix materials to decouple the filaments, and reduction of filament size to reduce losses in individual filaments. In [10] it was concluded that MgB_2 wires need to be fully decoupled and the filament size needs to approach the 10 μm level to meet the ac loss target.

Although the route is known, the development step has not yet been initiated. Promising research work on filament twisting has been done all down to twist pitches of 2.5 mm [11-13], although the shortest twist pitches result in significant critical current, I_c, degradation. Also, filament size has been reduced down to 10 μm [11, 14]. These achievements need to be combined and realized in an industrial setting to obtain wires with acceptable current densities, losses and cost.

The development of a low loss wire will include several steps where matrix materials, twisting and filament size will be changed, combined and tested to obtain a robust and industrial feasible conductor. In the wire development work it is important to have a solid understanding of the loss mechanisms. Although the theory of ac losses in multi-filamentary wires generally is well documented, e.g. in [15], there are a few aspects to clarify.

In this article, we describe the coupling current mechanism with a phenomenological approach, and we use it to discuss the behaviour of losses measured on short, non-twisted multi-filamentary samples of different lengths. Furthermore, the short sample data are used to estimate the influence of twisting for the particular wire architecture.

2. Ac loss mechanisms in multi-filamentary superconductors

2.1. Hysteresis losses

Hysteresis losses occur under ac operation in all superconductors of practical use as the magnetic field irreversibly penetrates the superconductor. The mechanism is often described in terms of the critical state model [16, 17]. Magnetic field enters the superconductor in the form of vortices. Inside the superconductor, the pinning force prevents the vortices from floating freely, and they become distributed with a higher concentration closer to the surface according to,

$$\left|\nabla \times \mathbf{B}\right| = \mu_0 J_c , \tag{1}$$

where **B** is the magnetic flux density and J_c the critical current density. The use of J_c becomes clear considering that a higher current density, J, would lead to losses in the superconductor, and a J lower than J_c would allow for more vortices to enter and to build up the gradient (1). Hence, the current density inside the superconductor is either J_c or zero.

When the field is reversed, the vortices start leaving at the surface, maintaining the relationship (1), resulting in a history dependent distribution of vortices inside the superconductor.

The corresponding hysteresis losses for superconductors exposed to a time-varying magnetic field depend on the shape of the superconductor. For a round superconductor with an ac magnetic field applied perpendicular to the axis of the superconductor, relevant for the measurements in section 3, the losses per unit volume, P_m, become [18],

$$P_m = \begin{cases} \dfrac{\omega}{2\pi}\dfrac{4B_a^3}{3\mu_0 B_p}\left(2-\dfrac{B_a}{B_p}\right) & for \quad B_a \le B_p \\ \dfrac{\omega}{2\pi}\dfrac{4B_a B_p}{3\mu_0}\left(2-\dfrac{B_p}{B_a}\right) & for \quad B_a \ge B_p \end{cases}, \tag{2}$$

where B_a and ω is the amplitude and angular frequency of the applied field, and B_p is the penetration field, equal to the applied field at which the vortices have reached the centre of the conductor, and $\left|J\right| = J_c$ throughout the superconductor. B_p can be expressed as $2\mu_0 J_c r/\pi$, where r is the radius of the superconductor. Note that for $B_a >> B_p$, as in many applications, the losses become proportional to ω, B_a, J_c and r.

2.2. Coupling currents

In multi-filamentary superconducting wires, electromagnetic coupling occurs between the filaments. Consider the conductor in figure 1 (left) with two superconducting filaments with a metal matrix in between. When the conductor is exposed to a time-varying magnetic field perpendicular to the plane of the paper, shielding currents may flow, as indicated by arrows, in the superconducting filaments and cross the metal matrix at the ends to cancel the magnetic field inside the loop. We call these currents coupling currents, and they give rise to ohmic losses when passing through the metal matrix.

These losses have an analogy with eddy current losses occurring in metals. However, whereas eddy currents encounter a certain electrical resistance in their entire loop, the coupling currents can build up over a long distance and only face the transverse resistance through the metal matrix at the ends of the loop. Hence, whereas the driving voltage $\mathrm{d}\Phi/\mathrm{d}t$ increases with increasing length of the loop, the resistance of the loop does not. Consequently, the coupling currents and the corresponding coupling current losses, can be much larger than the eddy current losses.

The coupling currents can be reduced by reducing the area of the loop (reducing the enclosed magnetic flux Φ and thus the driving voltage) by twisting the filaments, as in figure 1 (right), and by increasing the resistivity of the matrix material.

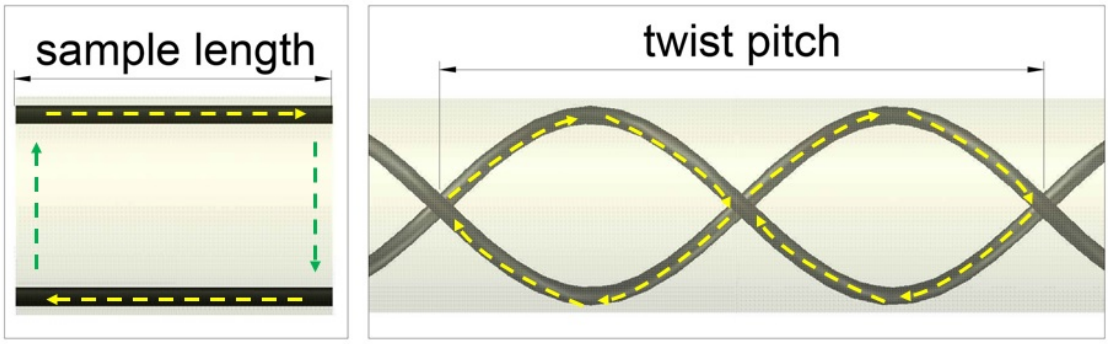

Figure 1. Coupling currents, represented by dashed arrows, in a non-twisted sample (left) and in a twisted sample (right).

The coupling currents are well described in [15], and the coupling losses per unit volume, $P_{coupling}/V$, are derived for partly coupled filaments, and are for a sinusoidal applied magnetic field with angular frequency, ω, given by,

$$P_{coupling}/V = \frac{2B_a^2}{\mu_0}\frac{\pi\omega^2\tau}{(\omega^2\tau^2+1)} \quad , \tag{3}$$

where,

$$\tau = \frac{\mu_0}{2\rho_{et}}\left(\frac{L}{2\pi}\right)^2 \quad , \tag{4}$$

and where L is the twist pitch and ρ_{et} is the effective transverse resistivity.

Of the two wire parameters, L is usually well defined, whereas ρ_{et} varies not only with the resistivity of the matrix material, but also with the contact resistance between the superconductor and the matrix. In several studies, the contact resistance has been found to be significant for MgB_2 wires and to strongly vary between samples with different matrices [19-21].

In addition to the losses appearing in the metal matrix, the coupling currents influence the hysteresis losses. For wires with decoupled filaments, the hysteresis losses appear in each filament independent of the other filaments, and consequently, for $B_a >> B_p$ in (2) the losses become proportional to the filament radius, r_{fil}. On the other hand, for wires with fully coupled filaments, the losses become proportional to the radius of the wire, r_{wire}. Hence, for multi-filamentary wires, the coupling currents both yield ohmic losses in the metal matrix and increase the hysteresis losses.

Equations (3) and (4) deal with partly coupled filaments. This is the situation for low $B_a^2\omega^2L^2$. With $\omega^2\tau^2 << 1$, $P_{coupling}$ becomes proportional to ω^2. This frequency dependency is sometimes used to distinguish the coupling current losses from hysteresis losses, (2), which are proportional to ω. However, as the coupling currents also influence the hysteresis losses, the situation may become somewhat more complicated.

2.3. Phenomenological explanation of coupling currents

In this work, we concentrate on the magnetic field region of primary interest for applications, namely $B_a > B_p$ for both a single decoupled filament and a fully coupled wire, corresponding to the lower equation of (2). This region is important from the application point of view in the development of low ac loss wires and has implications for measurements on non-twisted wires.

We shall look at a simplified case to determine how the twist pitch, the angular frequency and the magnetic field strength relate to coupling currents, and to coupling and hysteresis losses.

Consider again figure 1 (right) with two twisted filaments. The induced voltage, v, over one loop (half the twist pitch) is $-d\Phi/dt$, where Φ is the enclosed flux. For a sinusoidal

magnetic field $B = B_a \sin \omega t$, v becomes proportional to $rL\omega B_a \cos \omega t$, where r is the radius of the wire.

We will then find the relationship for the coupling current, $I_{coupling}$, passing in the loop consisting of the two filaments and the crossings through the metal matrix. We assume that the coupling current is limited by the resistance in the loop (and not the inductance), in fact corresponding to $\omega^2\tau^2 << 1$ in (3). The current then becomes v/R, where R is the resistance of the loop, which is approximately proportional to ρ_{et}/L (again disregarding the shape of the cross-section) for relatively short L where the current uses a large part of the transverse cross-section to pass between filaments. We should note, however, that this reasoning applies only up to $I_{coupling} = I_c/2$, where I_c is the critical current, since that current saturates the superconducting filament, corresponding to full coupling. Hence,

$$I_{coupling} \propto \frac{rL^2\omega B_a}{\rho_{et}} \cos \omega t \quad \text{for } I_{coupling} < I_c / 2 , \tag{5}$$

and,

$$I_{coupling} = I_c / 2 \quad \text{else.} \tag{6}$$

A higher $L^2\omega B_a$ leads to eddy currents, which normally are significantly lower as they are limited by the resistance in the entire loop. A typical behaviour is shown in figure 2, with a supressed peak for currents larger than I_c / 2. The traditional eddy currents are left out of the following treatment.

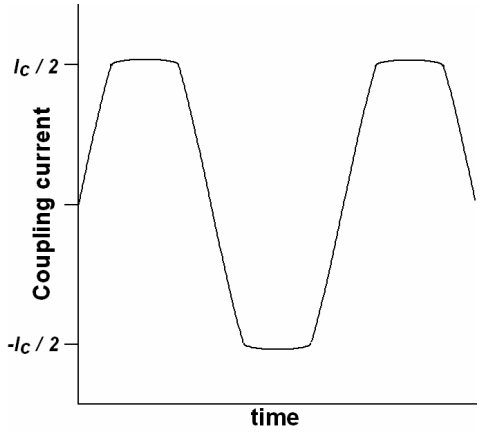

Figure 2. Suppressed peak of the coupling current when $I_c/2$ (full coupling) is reached. As the current is limited by the resistance in the loop, only a small traditional eddy current will add above $I_c/2$.

We now express the corresponding losses per unit length, $P_{coupling}/L$, where we set the length equal to the twist pitch, dealing only with full loops of the coupling currents. The losses in one loop are $RI_{coupling}^2$, with $R \propto \rho_{et} / L$ as before. Combined with (5) and (6) this yields,

$$P_{coupling} / L \propto \frac{r^2L^2\omega^2B_a^2}{\rho_{et}} \qquad \text{for } I_{coupling} < I_c/2 , \tag{7}$$

and,

$$P_{coupling} / L \propto \frac{\rho_{et}}{L^2} \qquad \text{otherwise.} \tag{8}$$

We see that for partly decoupled filaments, (8), the relationship coincides with (3) as expected (keeping the assumption $\omega^2\tau^2 << 1$ in mind). For fully coupled filaments, (8), the losses are independent of ω and B_a, whereas they are inversely proportional to L^2 (while the coupling current is constant, the resistance in the loop decreases linearly with L and the losses

are expressed per unit length). It should be noted that we in (8) have made the approximation that the coupling current becomes $I_c/2$ throughout the period as soon as its peak value is $I_c/2$.

When examining the total losses, the coupling losses need to be combined with the hysteresis losses in (2). We remind that for $B_a >> B_p$ the following relationship is valid,

$$P_{hysteresis} / L \propto \omega B_a r \quad , \tag{9}$$

and we will use (7), (8) and (9) in the next section to illustrate the anticipated loss patterns in multi-filamentary wires.

2.4. Ac loss patterns

The expressions for the coupling losses and the hysteresis losses are drawn schematically as function of ω, B_a and L in figures 3-6. We vary one parameter at a time, and treat ω and B_a in the same graphs as they yield the same loss dependency.

In figures 3 and 4 the coupling losses are given for three ρ_{et}: $\rho_{et1} < \rho_{et2} < \rho_{et3}$. In both graphs we see the quadratic behaviour until the coupling current reaches $I_c/2$ and thereby saturates the filaments. At higher B_a or ω in figure 3, the losses are constant, whereas for higher L the losses in figure 4 decreases inversely with L squared. Hence, for an infinitely long twist pitch, corresponding to a non-twisted wire, the coupling losses approach zero. The resistivity behaviour shows that a higher ρ_{et} results in a "later" increase in coupling losses, but with a higher end value (figure 3) or peak value (figure 4). A high ρ_{et} reduces the coupling current and ω, B_a or L need to be higher for the coupling current to reach $I_c/2$. However, at that point and above, independent of B_a and ω, the coupling current is constant, and the coupling losses becomes proportional to the resistance in the loop and hence to ρ_{et}.

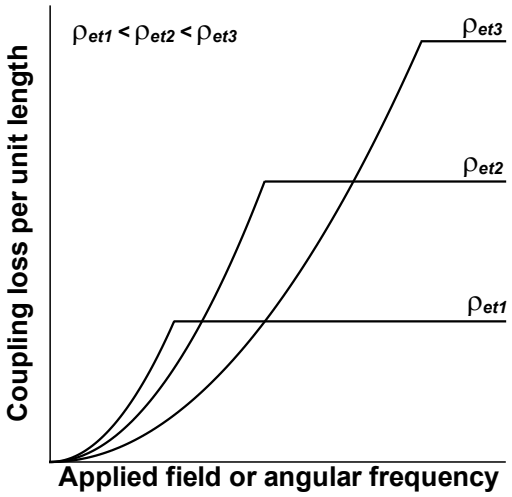

Figure 3. Coupling current loss per unit length as function of B_a or ω.

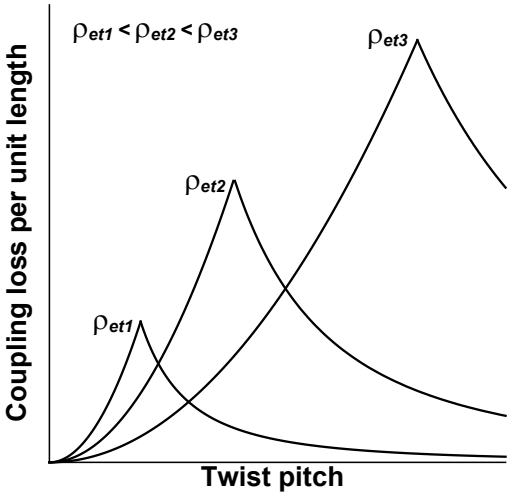

Figure 4. Coupling current loss per unit length as function of L.

The hysteresis loss follows another pattern, although linked to the coupling currents. At low ω, B_a and L, the filaments are decoupled (practically no coupling currents). In figures 5 and 6 the hysteresis loss for fully decoupled and fully coupled filaments (corresponding to no coupling currents and coupling currents equal to $I_c/2$, respectively) are marked with dashed lines. As ω, B_a or L increase, coupling currents increase and the hysteresis loss curve moves from the curve for decoupled filaments to the one for coupled filaments. For a low ρ_{et}, the shift from decoupled to coupled filaments occurs at lower ω, B_a or L and the hysteresis loss increases more rapidly than for higher ρ_{et}, until the filaments are fully coupled and the hysteresis loss becomes proportional to ω and B_a (figure 5), and independent of L (figure 6).

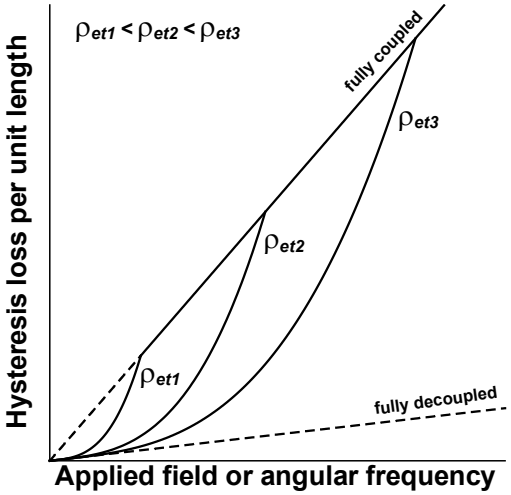

Figure 5. Hysteresis loss per unit length as function of B_a or ω.

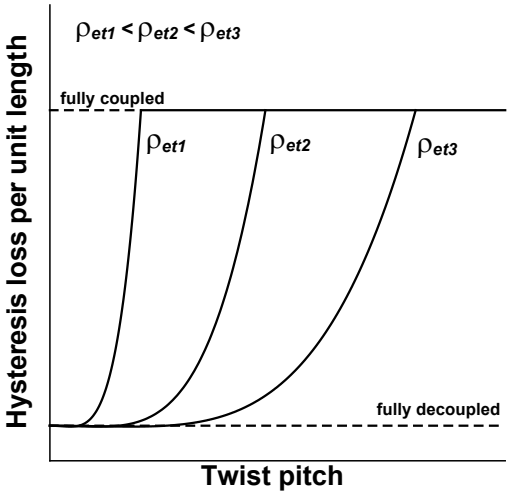

Figure 6. Hysteresis loss per unit length as function of L.

3. Experimental

3.1. MgB_2 samples

A round MgB_2 conductor with 19 filaments embedded in a titanium matrix was used in the experiments, see figure 7. The conductor was manufactured by Columbus Superconductors for research purposes. The diameter was 1.14 mm, the total area 1.01 mm^2 and the fill-factor 25%.

From one length of the conductor, six pieces were cut, placed in a mold and casted in Stycast 2850 epoxy. The samples were then carefully sanded about 4 mm from the ends to remove parts potentially mechanically damaged from cutting. The remaining sample lengths were 3, 4, 7, 12, 29 and 50 mm.

These sample lengths can be converted to equivalent twist pitches. Consider figure 1, the area enclosed by the current loop in the twisted conductor is about one third (or more precisely one over π) of the loop of a corresponding non-twisted conductor of length L [22]. Hence, an equivalent twist pitch becomes three times the sample length, and consequently the equivalent twist pitches in this study becomes 9, 12, 21, 36, 87 and 150 mm.

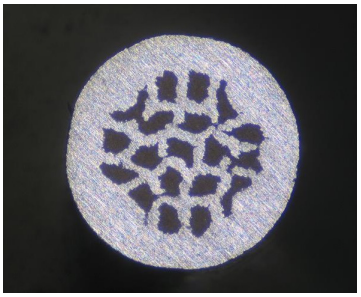

Figure 7. Cross-section of the MgB_2 sample [10].

3.2. Measurement method

The losses were measured calorimetrically with a system described in detail in [23]. Here a summary is given.

The samples were placed in vacuum on a sample holder thermally connected to the cold head of a cooling machine. Together with the samples, thin copper wires were bifilarly wound and used as thermometers. An ac magnetic field was generated over the samples by a current

in a set of coils placed outside the vacuum chamber. The magnetic field was on for durations of 5 - 40 s and resulted in losses in the samples and consequently temperature increases.

The obtained temperature increases were calibrated by measuring the temperature increases due to known power inputs to high ohmic wires also wound together with the samples.

4. Results and discussion

Depending on conductor architecture, including matrix material and not the least the superconductor-to-matrix contact resistance, either of the loss mechanisms above, coupling current loss or hysteresis loss, may dominate. In figure 8 the losses of the samples investigated in this study are plotted against frequency. The losses are to a first approximation proportional to the frequency, indicating that hysteresis is the dominant loss mechanism (compare with figures 3 and 5). When taking a closer look by plotting the energy loss per cycle, as in figure 9, the losses for the equivalent twist pitches of 36, 87 and 150 mm are rather constant (although with some scatter), indicating that in these samples the filaments are practically fully coupled. The losses for the shortest samples with equivalent twist pitches of 9 and 12 mm, on the other hand, reveal small increases of energy losses per cycle, as expected for conductors with small coupling currents (compare figure 5, assuming hysteresis losses to be dominant).

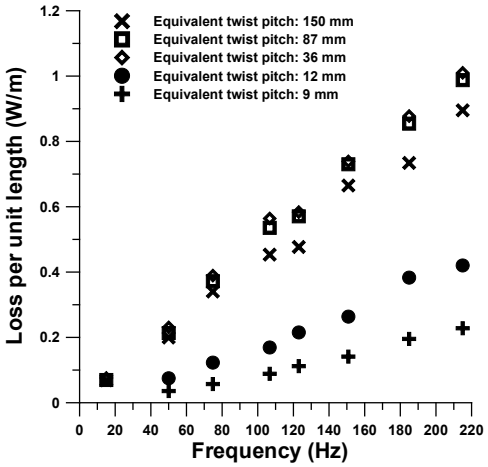

Figure 8. Measured losses as function of frequency for different equivalent twist pitches. The peak applied magnetic field was 100 mT and the temperature 32.5 K.

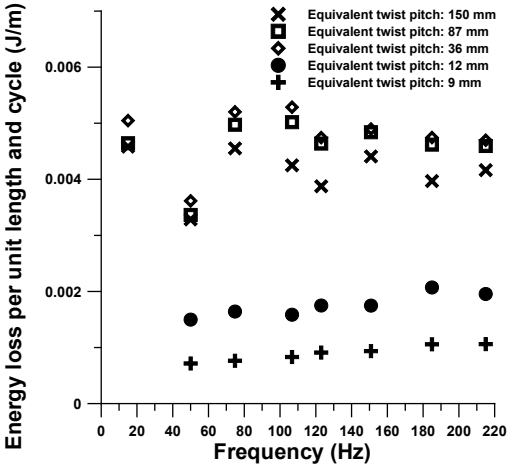

Figure 9. Energy losses per cycle as function of frequency for different equivalent twist pitches. The peak applied magnetic field was 100 mT and the temperature 32.5 K.

The impact of the sample length and equivalent twist pitch are maybe better illustrated in figure 10, where the losses are plotted against equivalent twist pitch. This graph should be compared to figures 4 and 6. The losses increase up to an equivalent twist pitch of approximately 36 mm, and thereafter the losses are rather stable or even reduce for the two highest applied magnetic fields. This behaviour again corresponds to a hysteretic dominance of the losses (compare with figure 6). The small decrease at large equivalent twist pitches may be attributed to a decrease in coupling current loss, as in figure 4.

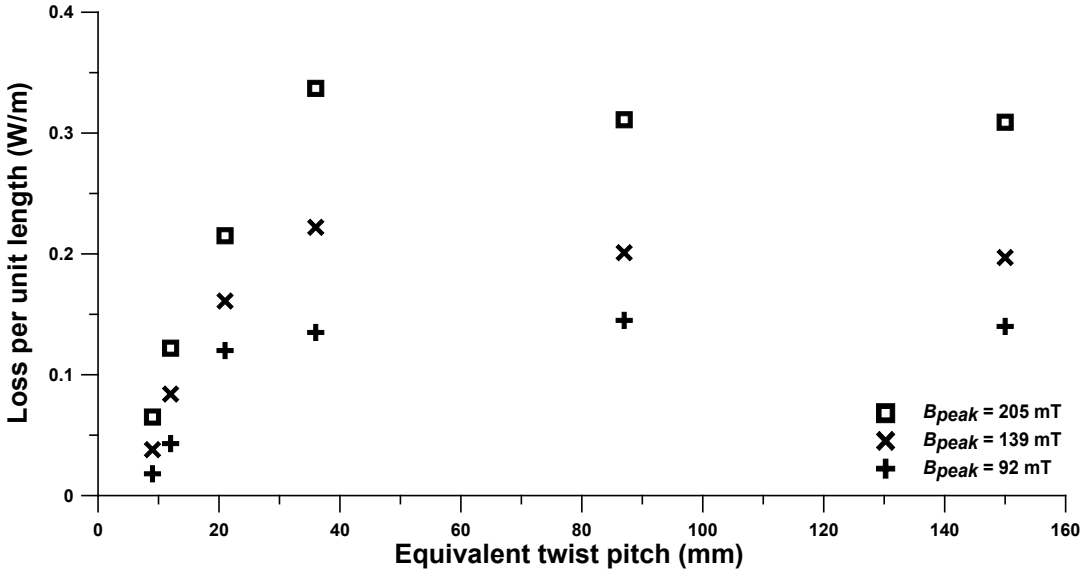

Figure 10. Measured losses as function of equivalent twist for three different applied magnetic fields. The frequency was 50 Hz and the temperature 35 K.

In figure 10 it is also notable that the losses per unit length decrease dramatically for shorter sample lengths, i.e. when the losses go from being determined by the full width of the filament region to being determined by the width of the single filaments as for wires with electromagnetically decoupled filaments. For this particular wire, twisting is efficient all down to approximately 9 mm.

The knowledge of the influence of the sample length is of course important when interpreting the loss results of multi-filamentary superconductors. For the particular conductor studied here, measurements at 100 mT, 50 Hz, 35 K do not represent full length conductors for sample lengths below approximately 15 mm (equivalent twist pitches below 45 mm).

More generally, the sample length of a non-twisted conductor needs to be above the critical length, L_c, determining the length at which full coupling occurs, to represent a full length conductor. For the conductor in this study with the losses dominated by hysteresis, the sample length needs only to be just over L_c. However, in a conductor with large coupling losses, the sample length needs to be a few L_c, compare figure 4. Generally the dependency of L_c is given by [15],

$$L_c \propto \sqrt{\frac{I_c \rho_{et}}{\omega B_a}} .$$

Hence, when investigating a non-twisted conductor with high critical current or high transverse resistivity, or measuring at low frequencies or low magnetic fields, the critical length can be significant.

For twisted conductors with twist pitches in the range or below L_c, the sample length needs to be at least a few twist pitches for the edge effect from cutting (which reduces the enclosed area for the coupling currents in the outermost half loops) not to significantly influence the results.

The hysteresis losses were dominant in the conductor under investigation in this study. In other conductors under different conditions, coupling currents have clearly been shown to influence the losses in MgB_2 wires. E.g. in [24], the ac losses in a mono-filament and a 30-filament wire were compared and coupling losses showed a clear dominance in the 30-filament wire, whereas the losses in the mono-filament wire were purely hysteretic.

5. Conclusions

The coupling currents can be described by a phenomenological approach showing how the coupling currents give rise to loss in the metal matrix and influence the hysteresis loss in multi-filamentary superconductors. With a proper understanding of the mechanisms, the loss dependency on frequency, applied magnetic field and twist pitch (or sample length) can be used to distinguish between coupling loss and hysteresis loss.

Due to the coupling currents, the sample length becomes a parameter potentially negatively influencing the quality of ac loss measurements on short samples of MgB_2 wires. For non-twisted wires the sample length needs to be at least a few times the length yielding full coupling to ensure correct results.

By cutting non-twisted wires into pieces of different lengths, the twist pitch necessary to decouple the filaments can be estimated.

Acknowledgements

This research was supported in part by the Research Council of Norway and the industrial partners of the NOWITECH programme.

References

[1] Razeti M, Angius S, Bertora L, Damiani D, Marabotto R, Modica M, Nardelli D, Perrella M and Tassisto M 2008 *IEEE Trans. Appl. Supercond.* **18** 882-6
[2] Zhang D et al. 2011 *IEEE Trans. Appl. Supercond.* **21** 2100-3
[3] Sætre F, Hiltunen I, Runde M, Magnusson N, Järvelä J, Bjerkli J and Engebrethsen E 2011 *Supercond. Sci. Technol.* **24** 035010
[4] Runde M, Magnusson N, Fülbier C and Bührer C 2011 *IEEE Trans. Appl. Supercond.* **21** 1379-83
[5] Abrahamsen A B, Magnusson N, Jensen B B, Liu D and Polinder H 2014 *J. Phys.: Conf. Ser.* **507** 032001
[6] Sanz S, Arlaban T, Manzanas R, Tropeano M, Funke R, Kováč P, Yang Y, Neumann H and Mondesert B 2014 *J. Phys.: Conf. Ser.* 507 032040
[7] Nakamura T, Yamada Y, Nishio H, Kajikawa K, Sugano M, Amemiya N, Wakuda T, Takahashi M and Okada M 2012 *Supercond. Sci. Technol.* **25** 014004
[8] Kajikawa K, Uchida Y, Nakamura T, Kobayashi H, Wakuda T and Tanaka K 2013 *IEEE Trans. Appl. Supercond.* **23** 5201604
[9] Young E A, Bianchetti M, Grasso G and Yang Y 2007 *IEEE Trans. Appl. Supercond.* **17** 2945-8
[10] Taxt H, Magnusson N, Runde M and Brisigotti S 2013 *IEEE Trans Appl Supercond.* **23** 8200204
[11] Malagoli A, Bernini C, Braccini V, Fanciulli C, Romano G and Vignolo M 2009 *Supercond. Sci. Technol.* **22** 105017
[12] Kawagoe A, Sumiyoshi F, Fukushima Y, Wakabayashi Y, Mito T, Takahashi M and Okada M 2009 *IEEE Trans. Appl. Supercond.* **19** 2686-9
[13] Kovác P, Hušek I, Melišek T and Kopera L 2011 *Supercond. Sci. Technol.* **24** 115006
[14] Kovác P, Hušek I, Melišek T, Kopera L and Polák M 2013 *J. Supercond. Nov. Magn.* **26** 2109-14
[15] Wilson M N 1983 *Superconducting Magnets* Oxford University press, New York
[16] London H 1963 *Physics Letters* **6** 162-5.
[17] Bean C P 1964 *Rev. Mod. Phys*. **36** 31-9
[18] Cizek M, Campbell A M, Ashworth S P and Glowacki 1995 *Appl. Supercond.* **3** 509-20
[19] Zhou C et al. 2013 *Supercond. Sci. Technol.* **26** 025002

[20] Polák M, Demencik E, Husek I, Kopera L, Kovác P, Mozola P and Takács S 2011 *Physica* C **471** 389-94
[21] Holúbek T, Dhallé M and Kovác P 2007 *Supercond. Sci. Technol.* **20** 123-8
[22] Lindau S, Magnusson N and Taxt H 2014 *J. Phys.: Conf. Ser.* **507** 022016
[23] Taxt H, Magnusson N and Runde M 2013 *Cryogenics* **54** 44-9
[24] Kovác J, Šouc J, Kovác P, Hušek I and Gömöry F 2013 *Physica C* **495** 182-6